

外加磁场闪光对焊 20 钢焊接接头组织分析

陈海东, 马铁军, 张 勇, 张笑宇*

(西北工业大学 摩擦焊接陕西省重点实验室, 西安 710072)

摘 要: 以一对条形永磁体为磁场源, 对比并分析了相同工艺参数下外加磁场对 20 钢闪光对焊接头显微组织及力学性能的影响. 未加磁场接头焊缝存在铸造组织及大量氧化物夹杂, 热影响区较宽; 外加磁场接头焊缝无铸造组织, 形成等轴的铁素体、少量魏氏体及珠光体组织, 热影响区窄, 且晶粒长大不严重. 力学性能试验表明, 未加磁场试样断在热影响区, 呈脆性断口; 加磁场试样断在母材, 有明显的塑性变形, 且抗拉强度明显增大. 结果表明, 外加磁场能有效改善闪光对焊接头质量.

关键词: 闪光对焊; 磁场; 20 钢; 显微组织

中图分类号: TG453+.9 **文献标识码:** A **文章编号:** 0253-360X(2012)02-0109-04



陈海东

0 序 言

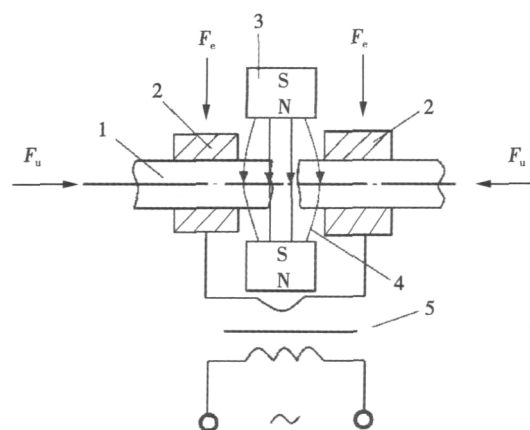
闪光对焊由于热效率高、焊接质量好、可焊金属和合金的范围广, 不但可以焊接紧凑截面, 而且可以焊接展开截面的焊件, 因此, 广泛应用于船舶、汽车、铁路、航空、航天等工业领域^[1]. 传统闪光对焊的工艺过程复杂, 很难形成封闭的焊口, 容易造成接头白斑、灰斑、裂纹、未焊透、氧化物夹杂等焊接缺陷, 而且在焊接后期焊接界面不可避免地存在少量液相结晶形成的铸造组织, 从而影响接头性能. 有效预防和消除焊接缺陷, 改善接头组织是提高焊接接头质量的关键. 人们过去通常通过改进焊接过程、规范工艺参数来预防和消除缺陷^[2]. 但这些方法耗时耗力, 经济成本较高, 其结果也未必见效.

在熔焊中, 利用外加磁场对焊接中熔滴过渡、熔池金属的流动、熔池的结晶形核及结晶生长等过程进行有效地干预, 能够使焊缝金属的一次结晶组织细化, 减小化学不均匀性, 提高焊缝金属的塑性和韧性, 降低结晶裂纹和气孔的敏感性, 从而提高焊缝金属的性能, 全面改善焊接接头的质量^[3]. 在电阻点焊中, 外加磁场能够增大熔核直径、细化晶粒组织、降低缩孔缺陷敏感性、有效地提高焊接接头拉剪强度和延展性^[4,5]. 而在闪光对焊过程中加入磁场来改善焊接接头质量, 目前鲜有研究. 因此文中尝试把外加磁场应用于闪光对焊, 通过研究外加磁场对

闪光对焊焊接过程、接头显微组织以及力学性能的影响, 以期改善闪光对焊接头的质量, 优化闪光对焊工艺过程.

1 试验方法

试验装置的原理如图 1 所示 (F_c 为夹紧力, F_u 为顶锻力). 在焊件上下两侧分别安装两块永磁体. 磁力线从 N 极出发, 经过焊接区回到 S 极. 所用永磁体为 NdFeB35 稀土永磁体, 表面剩磁为 0.3 T, 大小为 60 mm × 20 mm × 8 mm, 镶嵌在不影响磁场分布的胶木板上.



1. 焊件 2. 夹钳电极 3. 永磁体 4. 磁力线 5. 阻焊变压器

图 1 外加磁场闪光对焊原理图

Fig. 1 Principle diagram of flash butt welding with external magnetic field

试验采用 UN1-25 型手动杠杆加压式对焊机, 焊接试样为直径 10 mm 的 20 钢棒材, 焊接方法采用预热闪光对焊方式, 焊接工艺参数如表 1 所示。

表 1 闪光对焊工艺参数

Table 1 Processing parameters of flash butt welding

预热次数 N (次)	次级空载电压 U_{20}/V	伸出长度 l/mm	闪光留量 $\Delta f/mm$	顶锻留量 $\Delta d/mm$
2~4	2.9	16	4.5	1.5

焊后从未加磁场和外加磁场每组各抽取 5 件试样, 使用 INSTRON-3382 万能材料试验机测试接头的抗拉强度, 取测量结果的平均值作为该工艺参数下焊态接头的平均抗拉强度; 将焊接接头沿轴向线切割并制作金相试样, 用 3% 的 HNO_3 酒精溶液腐蚀后在 OLYMPUS PMG3 型光学显微镜上观察焊接接头的金相组织。

2 结果分析讨论

2.1 外加磁场作用闪光对焊液体过梁的受力分析

闪光对焊开始时, 在接通电源后, 将两焊件逐渐移近, 在焊件间形成很多具有很小电阻的小接触点, 并很快熔化形成一系列液体金属过梁。外加磁场作用闪光对焊时, 液体过梁除了受到液态金属的表面张力 σ 、电磁收缩效应力 F_{em} 等, 还受到由磁场和焊接电流综合作用产生的安培力 F , 其受力如图 2 所示。在焊接过程中, 由于通过试样为 50 Hz 的交流电, 而外加磁场为永恒磁场, 故闪光阶段时的液体过梁受到的方向不断交替改变, 使得液体过梁往复振动。这不仅使液体过梁更利于爆断, 而且扩大清洗面积, 较未加磁场时提高清理效率, 使焊接试样端面加热更加均匀, 火口深度更浅。焊接时电流峰值测

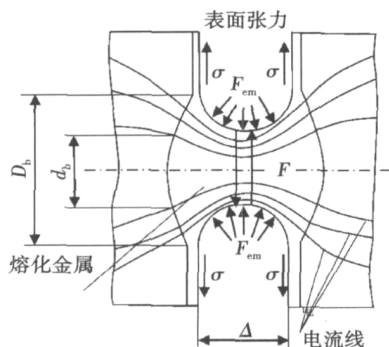


图 2 液体过梁受力示意图

Fig. 2 Force diagram of molten metal

量值如表 2 所示, 取 5 组电流峰值得平均值 $I = 5.5$ kA, 磁感应强度 $B = 0.3$ T, 则每毫米长度的液体过梁上所受到的最大安培力 F 约为

$$F = BIL = 0.3 \text{ T} \times 5500 \text{ A} \times 0.001 \text{ m} = 1.65 \text{ N}$$

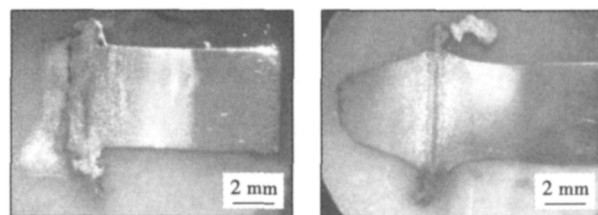
表 2 外加磁场下闪光对焊电流峰值

Table 2 Peak welding current of flash butt welding with external magnetic field

编号	电流峰值 I/kA
1	5.1
2	5.5
3	5.7
4	5.3
5	5.4
平均值	5.5

2.2 磁场对 20 钢闪光对焊接头组织的影响

未加磁场和加磁场下闪光对焊接头典型宏观形貌如图 3 所示。从图 3 中可以看出加磁场后焊接接头的热影响区宽度(约 5 mm)明显小于不加磁场焊接接头(约 3 mm)。这主要因为加磁场后, 液态金属过梁能尽快爆断, 并能较快排出焊接界面。液态金属的排除能带走大量的热量, 能够有效减小热影响区的范围, 并降低热影响区的温度梯度。因此外加磁场的焊件在较低的温度梯度作用下, 热影响区会小于未加磁场的焊接热影响区。



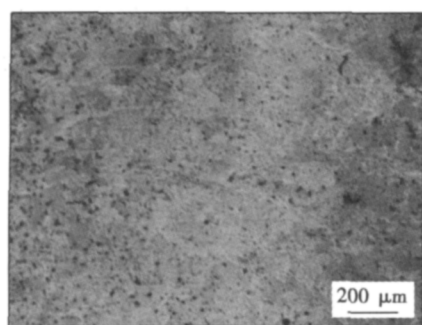
(a) 未加磁场接头宏观形貌 (b) 外加磁场接头宏观形貌

图 3 未加磁场和外加磁场接头宏观形貌

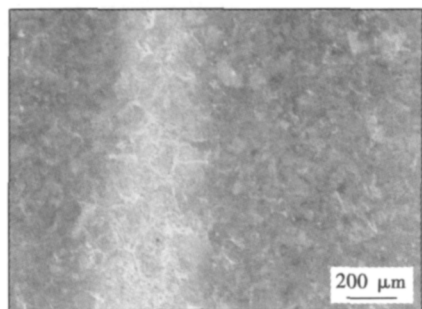
Fig. 3 Photo macrographs of different welded joints

未加磁场和外加磁场下接头焊缝区显微金相组织如图 4 所示。由图 4 可看出, 未加磁场时, 焊缝中有明显树枝状晶, 即铸造组织, 说明焊缝中有熔化金属尚未被完全挤出, 存在铸造组织及大量氧化物夹杂。外加磁场后, 在外加安培力、表面张力、电磁收缩效应力等因素共同作用下, 熔化金属被较快地挤出焊接界面, 从而有效清除了界面的铸造组织, 使热影响区变窄。

图 5 为图 4b 焊缝区的高倍金相组织, 从图 5 可



(a) 未加磁场焊缝显微组织



(b) 外加磁场焊缝显微组织

图4 未加磁场和外加磁场焊缝显微组织

Fig. 4 Microstructure of different welds

以清楚看到,外加磁场后,焊缝区为较粗大的铁素体+少量魏氏体+珠光体组织,晶粒为等轴晶。这表明,焊缝区已经加热到奥氏体化温度且冷却速度较快。外加磁场后,安培力加快了液体过梁爆破,析出了大量的热,最终使焊口冷却速度更快。

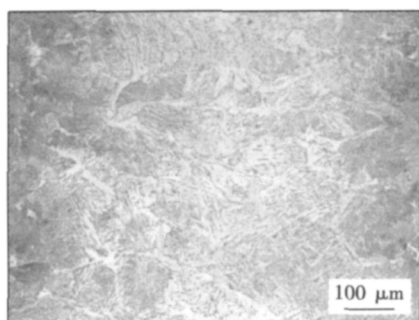
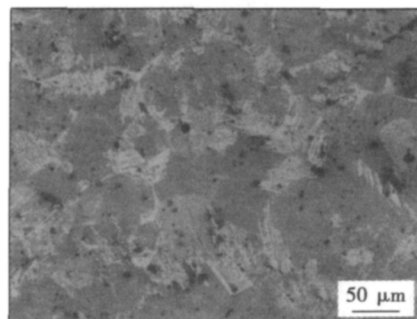


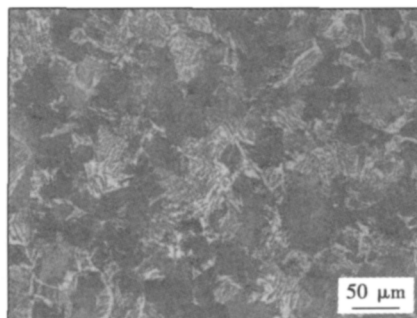
图5 外加磁场焊缝显微组织

Fig. 5 Microstructure of weld with external magnetic field

图6为未加磁场试样和外加磁场试样热影响区显微组织。从图6中可以看出未加磁场的晶粒较为粗大,且从晶界已析出较为明显的条状铁素体及块状铁素体,即已出现魏氏体组织。一般认为,魏氏体组织的出现降低了钢的冲击韧性,故未加磁场的闪光对焊接头的冲击韧性较低。而外加磁场的热影响区晶粒长大并不严重,晶粒较未加磁场略细。



(a) 未加磁场热影响区显微组织



(b) 外加磁场热影响区显微组织

图6 未加磁场和外加磁场热影响区显微组织

Fig. 6 Microstructure of different heat affected zones

在闪光对焊的顶锻阶段,会产生一定的塑性变形,能够促进再结晶的进行。其晶粒的大小与变形量、变形温度、应变速率、变形后停留时间以及原始奥氏体晶粒大小有关。大的变形量和低的加热温度,高的应变速率及细的原始晶粒尺寸都能促使晶粒细化。原始晶粒大小对再结晶过程的影响在变形量较小时更加明显,因为这时再结晶的核心主要集中在奥氏体晶界附近。当变形量大时,不仅晶界附近产生再结晶核心,晶内也易于产生再结晶核心,此时奥氏体晶粒的大小对再结晶后晶粒尺寸的影响就会逐渐减弱。在试验中,整个焊接过程都在外加恒定磁场的作用下完成。资料表明^[6],恒定磁场会影响低碳锰铌钢奥氏体向铁素体与珠光体转变的过程,磁场引起的高温钢辐射散热系数增大是导致晶粒细化的主要原因之一。在稳定磁场中低碳钢磁导率较大,磁场产生的晶粒细化作用会使组织的均匀度提高,这可能是由于磁场作用在试样上的安培力阻碍晶界移动,奥氏体晶粒长大较慢,导致晶粒较细。试验中晶粒细化不是很明显,这可能是由于外加磁场的磁感应强度较小,所产生安培力的作用不明显所致。

2.3 磁场对20钢闪光对焊试样拉伸性能的影响

对未加磁场与外加磁场的焊件每组各抽取5件试样,分别进行了拉伸试验,试验结果如表3所示。

从表 3 中可以看出,外加磁场试样的抗拉强度明显增大,其平均值提升了约 9.67%。磁场作用下焊接试样 2 和试样 5 的抗拉强度与同组试样的抗拉强度相差较多,这可能是由于使用手动杠杆加压机对焊机时,焊接过程中的人为因素影响较大。

表 3 试样拉伸试验强度极限
Table 3 Ultimate tensile strength of samples

试样	未加磁场焊接试样抗拉强度 R_{m1} /MPa	外加磁场焊接试样抗拉强度 R_{m2} /MPa
1	413.8	541.1
2	407.3	443.4
3	469.8	528.4
4	453.1	515.7
5	489.7	421.2
平均值	446.74	489.96

拉伸断口如图 7 所示。从图 7a 中可以看出,未加磁场试样断口垂直于正应力方向,较平坦,齐整,端口有金属光泽,在光线下可看到断面中颗粒状的小面闪闪发光。这是典型的脆性断裂断口,断在热影响区。由图 7b 可见,外加磁场试样断口是典型的杯锥状断口,断在母材。在此拉伸试验中出现了低碳钢拉伸时典型的颈缩现象,有明显的塑性变形,表明接头的抗拉强度已接近母材水平。

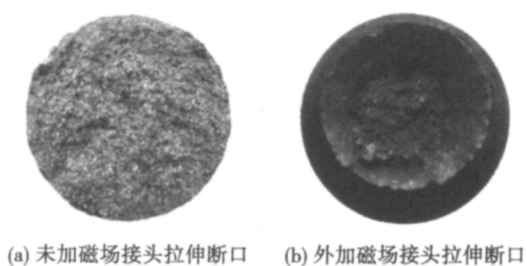


图 7 未加磁场和外加磁场的典型拉伸断口形貌
Fig. 7 Fracture appearance of tensile test specimens

在电磁作用下,焊接接头的力学性能会明显提高。这是由于焊接接头力学性能的变化是由微观组织的改变引起的。磁场作用使接头的晶粒细化,改变了晶粒方向,等轴晶的出现,组织缺陷的减少都有助于提高接头的力学性能。此外,在有电顶锻的过程中,焊接接头内的金属会受到周期性力的作用,使得材料内部微区应力状态随之发生变化,从而导致金属内部微区塑性变形而产生应力松弛,减少残余

应力,而且焊后焊接接头会在磁场作用下进行再结晶,这对接头的力学性能也有一定的提高作用。

3 结 论

(1) 外加磁场闪光对焊接头与未加磁场闪光对焊接头相比,焊缝中未见铸造组织及氧化物夹杂,主要为等轴的铁素体、少量魏氏体及珠光体组织,热影响区较窄且晶粒略细,抗拉强度及塑性明显提高。

(2) 外加磁场闪光对焊过程中,液体过梁在交变安培力的作用下扩大了清理面积,提高了清理效率,使接头界面加热更加均匀;过梁爆破后产生的火口深度较浅,液态金属容易被充分挤出,从而改善了接头组织性能。

参考文献:

- [1] 毕惠琴. 焊接方法及设备(第二分册). 电阻焊[M]. 北京: 机械工业出版社, 1981.
- [2] 黄华刚, 王克争, 何方殿, 等. 闪光对焊接头金相组织、性能和工艺关系的研究[J]. 焊接, 2000(11): 11-13.
Huang Huagang, Wang Kezheng, He Fangdian, *et al.* A study on the relationship between metallography structure, joint performance and welding process of flash butt welding[J]. Welding & Joining, 2000(11): 11-13.
- [3] 江淑园, 陈焕明, 刘志凌. 磁控技术在焊接中的应用及进展[J]. 中国机械工程, 2002, 13(21): 1876-1879.
Jiang Shuyuan, Chen Huanming, Liu Zhiling. Application and progress of magnetic control technology in welding[J]. China Mechanical Engineering, 2002, 13(21): 1876-1879.
- [4] Li Yongbing, Shen Qi, Lin Zhongqin, *et al.* Quality improvement in resistance spot weld of advanced high strength steel using external magnetic field[J]. Science and Technology of Welding and Joining, 2011, 16(5): 465-469.
- [5] 杨思乾, 马铁军, 张 勇. 多脉冲点焊与磁控制点缝焊技术及其现状[J]. 电焊机, 2005, 35(12): 36-38.
Yang Siqian, Ma Tiejun, Zhang Yong. Multi-pulsed spot welding and magnetic controlled AC spot/seam welding[J]. Electric Welding Machine, 2005, 35(12): 36-38.
- [6] 冯光宏, 周少雄, 杨 钢, 等. 稳恒磁场对低碳锰铌钢晶粒细化的影响[J]. 钢铁研究学报, 2000, 12(4): 27-30.
Feng Guanghong, Zhou Shaoxiong, Yang Gang, *et al.* Effect of stable magnetic field on grain refinement of low carbon Mn-Nb steel[J]. Journal of Iron and Steel Research, 2000, 12(4): 27-30.

作者简介: 陈海东,男,1987 年出生,硕士研究生。主要从事电阻焊设备及工艺方面研究工作。Email: haidongch@gmail.com

通讯作者: 马铁军,男,副教授。Email: matiejun@nwpu.edu.cn

na; 2. State Key Laboratory of Gansu Advanced Non-ferrous Metal Materials, Lanzhou University of Technology, Lanzhou 730050, China) . pp 93 – 96

Abstract: A new method of monitoring weld formation by means of binocular stereo vision is put forward. First, the images of weld formation were collected from joints surface on the vision system. The images were pretreated for gray balance and Gauss filter before image segmentation. Second, edges of weld formation were precisely extracted from the binary images by means of dynamic threshold segmentation and morphological approach of expansion and corrosion. On the basis, a method to measure weld length, weld width, weld height and other weld formation parameters was explored. At last, the actual verification results showed that standard deviation of weld width s_w , standard deviation of weld height s_H , and transition angel α_L and α_R could be made as quantitative indicators of evaluating weld formation.

Key words: submerged arc welding seam; weld formation; dynamic threshold segmentation; binocular stereo vision

Three-points welding analysis for compressor upper flange with different structures XIA Weisheng¹, WANG Ke^{1,2}, ZENG Zhijian², XIE Lichang², WU Fengshun¹ (1. State Key Laboratory of Material Processing and Die & Mould Technology, Huazhong University of Science & Technology, Wuhan 430074, China; 2. Zhuhai Lingda Compressor Co. Ltd, Zhuhai 519015, China) . pp 97 – 100

Abstract: The finite element model of the three-points welding processes for the condition compressor upper flange and its case was developed. The ANSYS software was applied. The temperature distributions of the three structures such as pierced, non-pierced and composite were simulated. Based on the temperature results, the relevant welding deformation were simulated by indirect coupling method. These deformations for the upper flange with different structures were compared and analyzed. The model was validated by the experimental welding results. Both the simulation and experimental results showed that the welding deformation of pierced upper flange was maximum. The deformation of the non-pierced was lower than that of the composite. Hence, the non-pierced upper flange was beneficial to decrease the welding deformation of condition compressor.

Key words: condition compressor; upper flange; three-points welding; welding deformation; finite element simulation

Analysis on microstructure and friction wear performance of chromium carbide/Ni₃Al composite surfacing layer AN Tongbang^{1,3}, GONG Karin², LUO Heli¹, PENG Yun¹, ZHU Xiaoyun³, TIAN Zhiling¹ (1. Central Iron & Steel Research Institute, Beijing 100081, China; 2. Chalmers University of Technology, Gothenburg Se-412 96, Sweden; 3. Kunming University of Science and Technology, Institute of Materials and Engineering, Kunming 650093, China) . pp 101 – 104

Abstract: Microstructure of chromium carbide reinforced Ni₃Al-based matrix composite coating prepared by argon tungsten-arc welding was investigated with optical microscope, scanning electron microscopy (SEM), electron probe micro-analysis (EPMA) and X-ray diffraction (XRD). The wear performance of the coating and cast iron of piston ring were tested by a Pin-on-Disc tribometer. The results indicated that the Ni₃Al-based matrix was formed during welding, a large number of fine carbide particles such as Cr₃C₂ and Cr₇C₃ dispersed in it; The particle of

Cr₃C₂ in welding wire was dissolved and re-precipitated during hardfacing. The re-precipitation of chromium carbide particle contains Fe, Ni elements and forms strong metallurgically bond with Ni₃Al-based matrix. Diffuse distribution of chromium carbide particles and Cr solid-solution in Ni₃Al-based matrix, makes the surfacing layer with higher hardness. The hardfacing layer shows excellent dry friction wear resistance and its friction coefficient is 0.23, lower than 0.39 which is the friction coefficient of piston material of vermicular graphite cast iron. The wear rate of hardfacing layer is only 43 percent of vermicular graphite cast iron.

Key words: chromium carbide; Ni₃Al; surfacing-welding; friction coefficient; wear resistance

Transient liquid phase diffusion bonding processing of Ni₃Al single crystal superalloy WU Song, HOU Jinbao, LANG Bo (Beijing Aeronautical Manufacturing Technology Research Institute, Beijing 100024, China) . pp 105 – 108

Abstract: By using KNi₃ alloy as filler, Ni₃Al single crystal superalloy were bonded through transient liquid phase bonding method. The changes of the microstructures of the bonded joints and the base metal in different holding time were analyzed. The mechanical properties of the bonded joints were tested. The results show that, for the TLP diffusion bonding joint at 1 240 °C for 12 h, a majority area of TLP bonding joint is the same as the matrix which consists of γ and γ' phases. Other area consists of the $\gamma + \gamma'$ eutectic phase and small block borides. γ' phase of base metal changes from largely cuboidal to irregular shape. Stress rupture strength of the TLP bonding joints at 1 000 °C reaches 90% of those of the standard base metal. During stress rupture, γ' phase rafted in bonding area were coarsening and irregular, which had some angles with the direction of stress rupture.

Key words: single crystal superalloy; transient liquid phase diffusion bonding; microstructure; rafted

Microstructural analysis of mild steel joint by flash butt welding with external magnetic field CHEN Haidong, MA Tiejun, ZHANG Yong, ZHANG Xiaoyu (Shanxi Key Laboratory of Friction Welding Technologies, Northwestern Polytechnical University, Xi'an 710072, China) . pp 109 – 112

Abstract: The influence of applied external magnetic field generated by a pair of bar permanent magnets on the microstructure and mechanical property of flash butt welded mild steel joint was analyzed. Cast structure and lots of oxide inclusions are found in the weld line without external magnetic field, and the heat affected zone (HAZ) is wider compared to the joint with magnetic field. Instead of cast structure, there are equiaxed ferrite with a small amount of Widmanstätten structure and pearlite in the weld line with magnetic field, and the grain coarsening in the HAZ is not obvious. In the tensile tests, the samples without external magnetic field fail in the HAZ with the brittle fracture, while the samples with magnetic field rupture in the base metal and obvious plastic deformation is found. The average tensile strength of the samples with magnetic field is higher compared with those without magnetic field. As a result, the joints by flash butt welding can be ameliorated through applying a magnetic field.

Key words: flash butt welding; magnetic field; mild steel; microstructure